Scientific Papers. Series E. Land Reclamation, Earth Observation & Surveying, Environmental Engineering. Vol. XV, 2026
Print ISSN 2285-6064, CD-ROM ISSN 2285-6072, Online ISSN 2393-5138, ISSN-L 2285-6064

# RESEARCH ON FREE SURFACE ENERGY DISSIPATION

**Nicolae ALBOIU, Daniel CORNEA, Georgiana Daniela VULPE**

Technical University of Civil Engineering Bucharest,
122-124 Lacul Tei Blvd, District 2, Bucharest, Romania

Corresponding author email: nalboiu@gmail.com

***Abstract***

*The paper is a general presentation of the studies undertaken as part of a research project focused on a solution used for energy dissipation applied to free surface currents. The research has involved a series of studies on special shaped artificial roughness elements proposed by the authors of the preset paper. Several placement patterns of these elements were tested. Based on the result, conclusions could be drawn regarding the effects that these elements and their placement have on the flow. Based on the results obtained experimentally, new research directions are possible to be developed, which are aiming at new building materials and maybe a more versatile implementation technology compared to the classical one.*

***Key words****: artificial roughness, energy dissipation, free surface current, water current.*

## INTRODUCTION

Dissipation of free surface kinetic energy is a necessity when certain flow conditions, specific to hydropower structures, gutters and channels adjacent to highways, roads and water transport systems used in agriculture are met. Uncontrolled discharge of water is a major threat for both the integrity of hydrotechnical and water transport infrastructure, and for the environment such as riverbeds, lake basins, and coastal areas. From the hydro engineering point of view, the general purpose of dissipating the kinetic energy of water streams is the reduction of riverbed erosion, structural protection and flood control by reducing the water velocity. Another category of problems for which energy dissipation is necessary is related to the ecology field. For example, the protection of aquatic habitats.

Several energy dissipation solutions were developed over time. Each situation has its own particularities. Broadly speaking, establishing the energy dissipation solution is related to the particularities of the flow and the generating cause that produces a high kinetic energy flow. Common, widely applied technical solutions for dissipating the kinetic energy of water streams are: *stilling basins* - reinforced pools placed at the base of structures like spillways, that use the hydraulic jump as main mechanism of dissipation; *stepped spillways* - a series of steps placed on the downstream face of the hydro-structure that divide the main high energy stream in small waterfalls will have a dissipative effect due to aeration and friction (Kiselev, 1988; Chanson, 2021; Mei et al., 2025); *baffle/chute blocks* (Figure 1) - obstacles placed in the channel to break the water stream reducing thus the water velocity; *bucket dissipators* - deflectors with a curved shape that lunch a water jet which energy is dissipated due to the resistance, water-air friction and finally as a result of the impact with the downstream water surface; c*heck dams* - small structures designed to break the riverbed slope reducing thus the stream velocity; *tumbling flow systems* - a sequence of concrete elements/obstacles or small steps which create falls and pools along steep channels (10 - 35% channel slope). Out of the above-mentioned solutions, as they increase the flow resistance, baffle blocks and chute blocks represent *artificial roughness* (Figure 1) methods of energy dissipation. Beside those two types of blocks, the artificial roughness category includes also *sills and ribs* - horizontal ridges built into the bed of the channel that act as a brake for the lower layer of water, and *rip-rap or boulders* - anchored rocks used in channels to enhance friction zones.

Although they have been studied and successfully applied for many years, these techniques continue to be of interest to researchers in the field of hydraulics. The

problems that remain open are related to the problem of cavitation, but also to the optimization of dissipative elements, a fact confirmed by recent research carried out in the last decade.

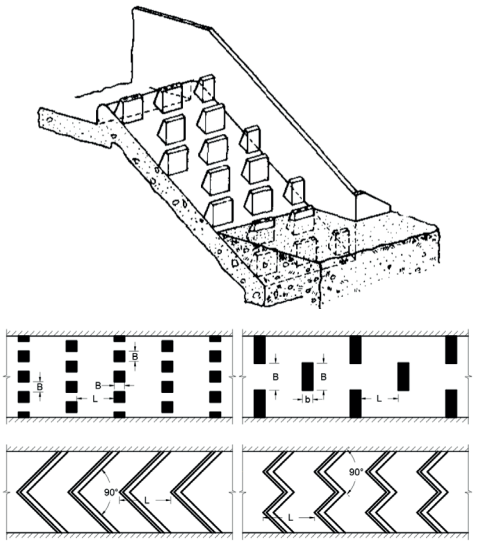



Figure 1. Example of baffle blocks (Peterka, 1984) and some increased artificial roughness types (Cioc, 1975) used for energy dissipation

Besides the presented solutions, a different but interesting dissipation method addressed to spillways, called *pre-aerated stilling basin spillway* (PSBS) is studied and presented in (Zhou et al., 2025).

Considering the technological evolution in the field of hydraulic phenomena research, both experimental and numerical (CFD), but also the evolution of building materials and execution technologies, the authors of this paper proposed a new shape of artificial roughness elements used for energy dissipation.

The research is focused on induced tumbling flow by using these elements. The development of the studies involved a succession of activities based on which the most efficient methods and approaches were used to draw valid conclusions regarding the behavior of the proposed roughness elements under operation conditions.

The research is a part of the *National Research Grants of the Technical University of Civil Engineering Bucharest GnaC ARUST 2024, DERA project, number TUCEB- No.1411/2025*.

## MATERIALS AND METHODS

To carry out the proposed research, both theoretical and experimental methods were considered.

*The theoretical studies* involved preliminary evaluations on which the future experimental research was developed. The subjects of interest were related on one hand to the main physical quantities used to describe and quantify free surface water streams and on the order hand to the potential effect of the roughness elements on a theoretical stream. Both evaluations were used to establish the future experimental framework and to provide a qualitative picture of the fluid flow kinetics in the presence of the artificial roughness elements.

For the numerical evaluation of the flow the well-known analytical relationships and the HEC-RAS software were used (Cioc, 1975; French, 1986). The qualitative relative effect of the roughness elements was evaluated prior to any test via the COMSOL Multiphysics CFD software. The analysis was based on a hypothetical scenario. Under this scenario four types of roughness elements were compared. The shape of the compared elements is shown in Figure 2.

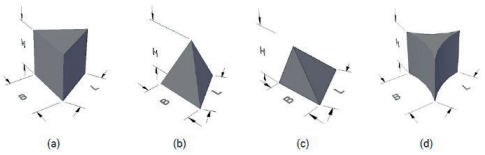



Figure 2. Shapes of the evaluated artificial roughness elements

All the four elements shown in figure 2 are considered 10 cm high (H) and 10 cm wide (B). The characteristics of the modeled domain are 1.5 m length and 1.2 m width. The artificial roughness elements were placed alternately as a single row, facing the water stream at 0.3 m downstream from the inlet of the domain. Considering the characteristics of the studied problem, a RANS k-ε turbulence model was used.

Based on the results of the qualitative, relative, evaluation, the shape depicted by image (d) was chosen for the future experimental tests (Figure 3).

The elements were made from plastic sheets cut on CNC machines and subsequently glued together. To obtain a uniform average roughness between the elements, the resulting pieces were wrapped in adhesive aluminum foil. Twenty-two central elements were placed in the flow field, and 4 lateral elements were placed near the channel walls.

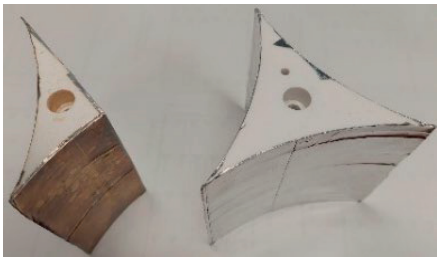


Figure 3. Lateral and central artificial roughness elements selected for the experimental study

*The experimental studies* were carried out in the „Dumitru Cioc" Hydraulics Laboratory (HL) part of the Technical University of Civil Engineering Bucharest (TUCEB).
To perform these experimental studies, some of the main infrastructure of the HL was used, namely the variable slope channel, the pumping station and the related hydraulic network.
The characteristics of the variable slope open channel are: a rectangular cross section, 1.20 m wide and 0.75 m depth (of which 0.65 m is the usable depth), the total length of the channel is 33.20 m, the maximum elevation difference at the downstream end, compared to the horizontal position, is 0.35 m that corresponds roughly to a channel slope of 1% (Figure 4).



Figure 4. The variable slope channel - „Dumitru Cioc" Hydraulics Laboratory; TUCEB

The pumping station is equipped with four centrifugal pumps, ensuring a maximum flow rate of 0.6 $m^3/s$.
The flow rate is measured using electromagnetic flowmeters placed on the laboratory water supply network pipes. The supply of the variable slope channel is ensured by two pipes connected to the tank placed at the upstream end. Each of these is equipped with a flow meter and a control valve. The diameters of these pipes are 200 mm and 250 mm, respectively.
To carry out the experimental study, a series of adjustments were necessary which mainly consisted of doubling the bottom of the channel and creating a well-defined experimental area. The solution to doubling the bottom was considered the only acceptable option for fixing the artificial roughness elements in a safe manner that would not affect the integrity of the channel. Three plastic plates were placed in the upstream area of the channel and fixed with metal strips to its walls. The total length occupied by these plates is 6.5 m. The first and last plates do not present any particularities. However, the central plate was provided with recessed nuts, their role is to ensure fixing of the roughness elements. The arrangement of the fixing nuts makes it possible to achieve a placement of the artificial roughness elements at a minimum distance of 10 cm on both main directions of the horizontal plane.
The theoretically obtained results regarding the flow characteristics were used as a starting point for the planning of future experiments. Thus, the precise experimental framework was established.
The measurements monitored the main physical quantities that are used for the description, characterization and classification of free surface currents, namely flow rates, depths and local velocities.
For flow rate measurements, the flow meters placed on the water supply pipes were used. The water depth was monitored using an ultrasonic probe, and the local velocity using an acoustic Doppler velocimeter (ADV) and, subsidiary, a Pitot tube connected to a pressure transducer (Figure 5).



Figure 5. Measuring equipment used

Due to the low water depth, a 2D side looking ADV probe was used. the acquisition frequency

of the measured values was set at 20Hz. To avoid measuring errors related to noise and sampling faults and post processing, several bibliographic works were consulted, including (Kazemi et al., 2021; Park & Hwang, 2021; Chen et al., 2024).

The first action aimed to establish the framework for the tests to be carried out. In this regard, the theoretical estimates initially made were experimentally verified. Based on these tests, the flow-depth-slope relationship which ensures the desired experimental framework was established.

First, to obtain high velocity values for the water stream the maximum possible slope ($i_{max}$) of the channel was set ($i_{max}$ = 1%). The experimental medium flowrate was Q = 0.096 $m^3/s$. The measured mean depth along the channel was $h_{med}$ = 0.10 m. For this setup, an unfavorable aspect that was observed was the deformation of the third bottom plate because of the lifting force generated by the water current.

The solution chosen to avoid this issue was to set a smaller slope for the channel and to increase the velocity of the water strictly in the first part of the experimental zone, by placing a sluice gate at the inlet section of the channel (Figure 6).

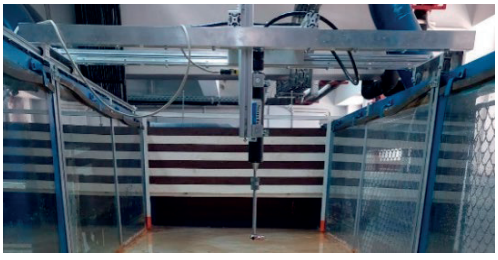


Figure 6. The sluice gate placed
at the upstream of the testing zone

After computation and experimental tests, the convenient experimental setup was established (Dumitrescu & Răzvan, 1972; French, 1986): the channel slope *i = 0.1%;* the experimental medium flow rate Q = 0.096 m3/s; the gate opening *a = 7 cm.* For the experiments a single arrangement and three different orientations (patterns) were considered (Figure 7).

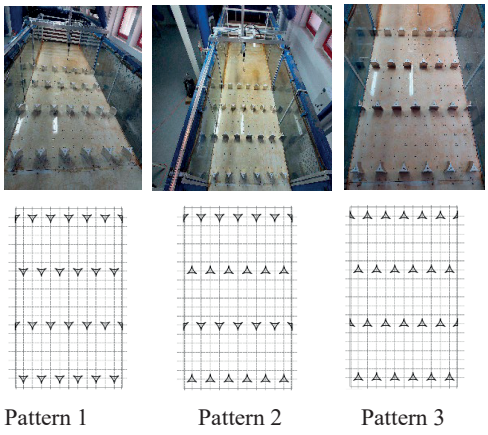



Figure 7. Patterns used for experimental test

The single arrangement for the three patterns is justified by the dissipation mechanism that is studied, namely tumbling flow.

For further reference of the studied arrangement, we will use the following names Pattern 1, Pattern 2 and Pattern, as shown in Figure 7, and for the "free" channel, i.e. without roughness elements, we will use the name Pattern 0.

Experiments carried out in the past by various researchers on alternatingly placed concrete cubes and the experience gained by applying this solution show, according to (Certousov, 1966; Dumitrescu & Răzvan, 1972; Morris & Wiggert, 1972; Peterka, 1984; Kiselev, 1988; Novak et al., 2005) referenced literature, recommended ratios between the height of the element and the depth of the current at the design flow rate and distances for placing the roughness elements in the direction of the current and transverse to it.

Although we proposed a new shape for the roughness elements, we considered these recommendations a rational starting point. However, a determined criterion was also the size of the area designated for mounting the roughness elements, this being used to the maximum extent. Considering the height of the elements, the longitudinal, the transversal spacing and the water depth, the studies were driven on a prototype (geometric scale coefficient $\alpha_l$ = 1).

## RESULTS AND DISCUSSIONS

*The CFD results* obtained on the modeling that assumes a hypothetical scenario, allowed a general qualitative analysis of the influence of the four roughness elements geometry. The conclusions are strictly valid within the assumptions and numerical conditions adopted. In the absence of experimental validation, the results cannot be considered from a quantitative point of view. Thus, they were used only as a starting point for choosing the geometry of roughness element used for future experimental tests.

The experimental tests were performed along the flow axis, tracking velocities at various depths for two relevant monitoring sections. The placement of those monitoring sections, $S_{ust}$ and $S_{dst}$, are upstream and respectively downstream the bottom plate where the roughness elements are fixed (Figure 8).



Figure 8. Measuring equipment placed at $S_{ust}$ and at $S_{dst}$

A first image of the effect generated by the three patterns compared to the "free" channel is plotted in Figure 9.

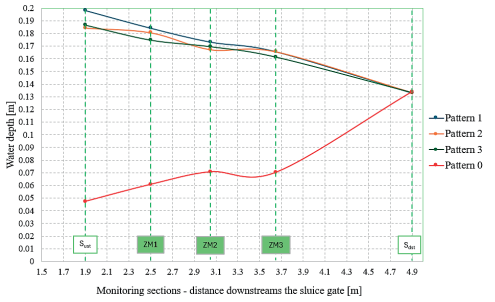



Figure 9. Comparative plot of the free surface shape

As shown in Figure 9, each of the Patterns P1, P2 and P3 are modifying the water depth along the experimental area. The water depth increases significantly in all the first three monitoring sections. In the last one, $S_{dst}$, the water reaches the same depth for all four patterns (Table 1).

Table 1. Water depth values along the experimental area

| Monitoring section | $S_{ust}$ | ZM1 | ZM2 | ZM3 | $S_{dst}$ |
|---|---|---|---|---|---|
| Water depth [m] | | | | | |
| Pattern 0 | 0.047 | 0.061 | 0.071 | 0.070 | 0134 |
| Pattern 1 | 0.198 | 0.184 | 0.173 | 0.166 | 0.133 |
| Pattern 2 | 0.184 | 0.181 | 0.167 | 0.166 | 0.133 |
| Pattern 3 | 0.187 | 0.175 | 0.170 | 0.161 | 0.133 |
| Water depth difference – Reference "Pattern 0" [m] | | | | | |
| Δ h1 | 0.151 | 0.123 | 0.102 | 0.096 | ≈0 |
| Δ h2 | 0.137 | 0.120 | 0.096 | 0.096 | ≈0 |
| Δ h3 | 0.140 | 0.114 | 0.099 | 0.091 | ≈0 |

After the $S_{dst}$ section the flow becomes uniform with a normal depth of roughly 0.16 m.

The presence of the artificial roughness generates a local resistance which influences the channel's flow rate. As the water depth rises upstream the artificial roughness elements, the orifice created by the sluice gate become submerged. Thus, the orifice head ($H_{orif}$) changes with respect to the degree of submergence. This fact is reflected in the flow rate (Table 2).

Table 2. Values influenced by orifice submergence

| Pattern | $h_{ust}$ | $H_{orif}$ | $Q$ |
|---|---|---|---|
| | [m] | [m] | [m$^3$/s] |
| 0 | 0.047 | 0.22 | 0.0955 |
| 1 | 0.198231 | 0.3 | 0.0950 |
| 2 | 0.184333 | 0.285 | 0.0947 |
| 3 | 0.186583 | 0.255 | 0.0945 |

The flow rate values shown in Table 2 are plotted in Figure 10 against orifice head ($H_{orif}$) by which the flow rate changes due to the head upstream the orifice are obtained.

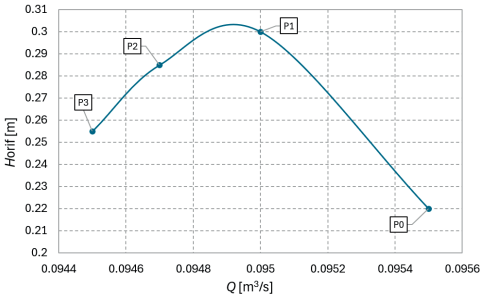



Figure 10. Flow rate curve Q($H_{orif}$)

Also, the flow rate plotted against the water depth in the $h_{uts}$ monitoring section, which is placed downstream the sluice gate, is useful to observe this influence (Figure 11).

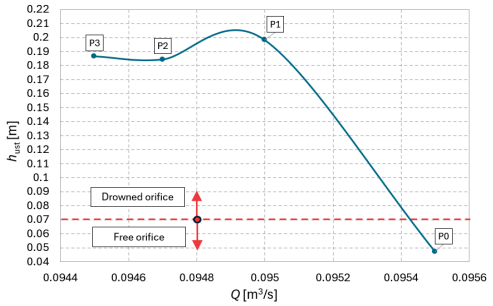



Figure 11. Flow rate curve Q($h_{ust}$)

Starting from the observation on the drowning effect of the gate orifice, the experiments on the dissipative effect generated by the three patterns were carried out at a same flowrate value, namely Q = 0.095 m3/s.

As the present paper focuses only on the whole ensemble of artificial roughness elements, the data obtained for the monitoring sections $S_{ust}$ and $S_{dst}$ are analyzed and discussed.

For Pattern 0 (Figure 9), the water depth is increasing significantly between $S_{ust}$ and $S_{dst}$. The shape of the water surface and the Froude number upstream ($Fr_1$ = 6.33) and downstream ($Fr$ = 0.36) are highlining a hydraulic jump. The flow upstream the testing area is supercritical and downstream the testing area is subcritical.

Thus, the goal of the artificial roughness is to reduce the kinetic energy of the water stream at $S_{ust}$ and to ensure a similar specific energy to the normal flow conditions one at $S_{dst}$. The graph in Figure 9 suggests the achievement of this goal.

A comparison between the values obtained for monitoring section $S_{ust}$ is shown in Table 3.

Table 3. Monitoring section $S_{ust}$ - values obtained for the main quantities

| Pattern | $h_{ust}$ [m] | $\Delta h_{ust}$ [m] | $V_{ust}$ [m/s] | $\Delta V_{ust}$ [m/s] | $KT_{ust}$ [m] | $\Delta KT_{ust}$ [m] |
|---|---|---|---|---|---|---|
| P0 | 0.047 | - | 1.815 | - | 0.168 | - |
| P1 | 0.198 | 0.151 | 0.338 | -1.477 | 0.006 | -0.162 |
| P2 | 0.184 | 0.137 | 0.510 | -1.304 | 0.014 | -0.154 |
| P3 | 0.187 | 0.140 | 0.368 | -1.446 | 0.007 | -0.161 |

The values shown in Table 3 for the four analyzed patterns are the water depth $h_{ust}$, the mean velocity $V_{ust}$ resulted from averaging the values obtained through local measurements and $KT_{ust}$ the specific kinetic energy value of the generalized Bernoulli equation. Also, the difference between a considered reference value, which corresponds to pattern P0, and the corresponding value obtained for the other three patterns are presented. The notations used are $\Delta h_{ust}$ for the obtained water depth difference, $\Delta V_{ust}$ for the mean velocity difference and $\Delta KT_{ust}$ the specific kinetic energy difference.

As shown in Table 1 and Table 3 the water depth increases due to the presence of any of the three patterns of the artificial roughness (P1, P2 and P3). Obliviously, this increase of the water depth generates a decreasing of the water velocity and consequently of the specific kinetic energy. The minus sign of those two differences is showing this decrease. The velocity decreases 81.37% for P1, 71.88 % for P2 of and 79.71% for P3. Also, a significant decrement is noticed for specific kinetic energy: for P1, 96.36%, for P2, 91.94% and for P3, 95.84%.

As a general conclusion, all the data obtained confirms the expected changes in the water surface profile for patterns P1 to P3. Namely, the presence of a high roughness area leads to rise in upstream water level and decrease in the downstream water level.

The analysis of the general effect produced by the presence of artificial roughness is driven by comparing the main quantities derived from the water depth and the water velocity measurements (Bekheet et al., 2025; Ghomri et al., 2023; Yang et al., 2025).

The first driven physical quantity was the difference of the total head corresponding to $S_{ust}$ and respectively to $S_{dst}$, for each of the three patterns of artificial roughness. This friction loss was obtained by applying the energy equation (the generalized Bernoulli equation) between the two monitoring sections. The results obtained are shown in Figure 12.

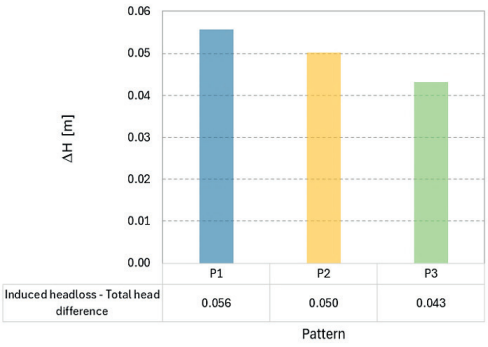



Figure 12. Fiction loss $\Delta H$ induced by the three patterns

As shown in Figure 12, pattern P1 induces a drop of the hydraulic head of 5.6 cm. Compared to this value, the drop generated by P2 is 10.71% less, and the third one, P3, 23.22% lower than P1.

Another way to quantify the dissipative effect between Sust and Sdst is by using the dissipated power (Figure 13).

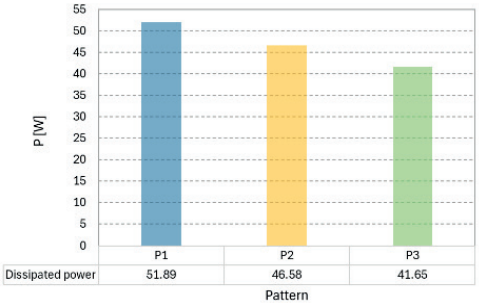



Figure 13. Dissipated power by the three patterns

The results obtained on the efficiency of each of the three patterns are plotted in Figure 14.

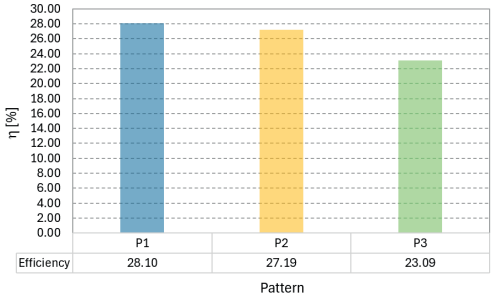



Figure 14. Efficiency of each of the three patterns

As shown in Figure 14, the most effective pattern is P1. Compared to P1, the dissipation efficiency decreases 3% for P2 and 17.83 % for P3.

## CONCLUSIONS

The experimental tests carried out in the „Dumitru Cioc" Hydraulics Laboratory, part of the Technical University of Civil Engineering Bucharest, are seen as a starting point for future tests.

The results obtained are considered encouraging for developing future research on the shapes proposed for the roughness elements.

The future possible research may follow two paths. The first one continues the hydraulic experimental tests with different flow rate values, diverse channel slopes and various distances between the artificial roughness elements. To obtain a complete image of the flow in the wake of the experimental area, transvers measurements at different depths are necessary. Also, the evaluation of turbulence like studies on turbulent kinetic energy and Reynolds stress provides important information about energy dissipation and is considered for future research.

A shortcoming of the experiments was the reduced number of available artificial roughness elements and consequently the low extent of the test area. Also, the lifting phenomenon of the bottom plates has dictated the maximum velocity value that can be used for the experiments (1.82 m/s). After correcting the previously mentioned aspects a comparative study, carried out in the same flow condition, on the behavior of the proposed artificial roughness elements and a classical shape like cubic elements is considered useful.

The second path that can be followed is related to the use of new materials for building the artificial roughness elements. New materials and new technologies are now available. A series of interdisciplinary studies involving the hydraulics laboratory personnel and the chemistry and building materials department of the TUCEB are considered of interest.

## REFERENCES

Bekheet, A. A., AboulAtta, N. M., Saad, N. Y., & Molla, D. A. (2025). Energy dissipation in stepped spillways: a comprehensive review of the recent research. *Innovative Infrastructure Solutions*, 10. 10.1007/s41062-025-02042-6.

Certousov, M. D. (1966). *Hidraulica. Curs special* [Hydraulics. Special course]. Bucharest, RO: Technical Publishing House.

Cioc, D. (1975). *Hidraulică* [Hydraulics]. Bucharest, RO: Didactic and Padagogic Publishing House.

Chanson, H. (2021). Hydraulics and Energy Dissipation on Stepped Spillways – Prototype and Laboratory Experiences. *Proceedings of the 2nd International Symposium of Water Disaster Mitigation and Water Environment Regulation*. Chengdu, China.

Chen, Y., Yang, W., & Lin, H. (2024). Reproducing the temporal averaging process of the acoustic Doppler velocimeter and assessing its impact on turbulence measurements. *Measurement*, 226. 114093. 10.1016/j.measurement.2023.114093.

Dumitrescu, D., & Răzvan, E. (1972*). Disiparea energiei și disipatori de energie* [Energy dissipation and energy dissipators]. Bucharest, RO: Technical Publishing House.

French, R. H. (1986). *Open-channel Hydraulics.* New York, USA: McGraw-Hill Book Company.

Ghomri, A., Lacheheb, S., & Djamaa, W. (2023). Effect of roughness on the characteristics of the hydraulic jump evolving into a rectangular channel of compound section. *Journal of Fundamental and Applied Sciences*, 13. 50. 10.4314/jfas.1300.

Kazemi, M., Khorsandi, B., & Mydlarski, L. (2021). Effect of Acoustic Doppler Velocimeter Sampling Volume Size on Measurements of Turbulence. *Journal of Atmospheric and Oceanic Technology*, 38. 10.1175/JTECH-D-20-0174.1.

Kiselev, P.G. (1988). *Îndreptar pentru calcule hidraulice* [Hydraulic Calculation Guide]. Bucharest, RO: Technical Publishing House.

Mei, J., Zhou, Y., Xu, K., Shu, Z., Gan, Q., Yu, Q., & Qian, J. (2025). Energy Dissipation on Inclined Stepped Spillways. *Water*, 17. 251. 10.3390/w17020251.

Morris, M.H., & Wiggert, J.M. (1972). *Applied Hydraulics in Engineering.* New York, USA: Ronald Press Company.

Novak, P., Moffat, A.I.B., Nalluri, C., & Narayanan, R. (2005). *Hydraulic Structures.* London, UK: Taylor & Francis.

Park, H., & Hwang, J.H. (2021). A Standard Criterion for Measuring Turbulence Quantities Using the Four-Receiver Acoustic Doppler Velocimetry. *Frontiers in Marine Science*, 8. 681265. 10.3389/fmars.2021.681265.

Peterka, A. J. (1984). *Hydraulic Design of Stilling Basins and Energy Dissipators. Engineering Monograph No. 25.* Denver Colorado, U.S: Department of the Interior Bureau of Reclamation.

Yang, J., Li, S., Farooq, U., & Helgesson, A. (2025). Energy Dissipation in Chute Spillway with Labyrinth Roughness Appurtenances. *Water*, 17. 3417. 10.3390/w17233417.

Zhou, Y., Huang, T., Xu, K., Mei, J., Jia, S., Yu, Q., & Qian, J. (2025). Hydraulic performance of a pre-aerated stilling basin: Experimental study. *PLOS ONE,* 20. 10.1371/journal.pone.0318191.